




Corrosion prevention of sintered Nd–Fe–B magnet by a phosphate chemical conversion treatment

Xia Ding, Xiu-Chun Wang, Kai-Hong Ding,
Sheng-Li Cui, Yong-Cong Sun, Mu-Sen Li* 

Received: 9 May 2014/Revised: 18 June 2014/Accepted: 5 June 2015
© The Nonferrous Metals Society of China and Springer-Verlag Berlin Heidelberg 2015

Abstract The corrosion-resistant coating formed on the surface of sintered Nd–Fe–B magnet by a phosphate chemical conversion (PCC) treatment was studied. The morphology, phase composition and thickness of the coating were investigated by field emission scanning electron microscopy (FE-SEM), energy-dispersive spectrometer (EDS), Fourier transform infrared (FTIR) spectrometer and coating thickness gauge. The corrosion behaviour of the phosphated magnet was evaluated by copper sulphate spot test, neutral salt spray test and electrochemical potentiodynamic polarization experiment. The magnetic properties of the phosphated magnet were also tested. The experimental results show that the phosphate coating has such characteristics as dense granular growth, uniform distribution and thickness range of 10–18 μm . The corrosion resistance of the magnet is significantly improved by phosphate coating without losing magnetic properties. Therefore, this highly efficient PCC was a good way for increasing the corrosion resistance of the sintered Nd–Fe–B magnets.

Keywords Nd–Fe–B magnet; Phosphate chemical conversion; Microstructure; Corrosion resistance

X. Ding, M.-S. Li*
Key Laboratory for Liquid-Solid Structural Evolution and Processing of Materials, Ministry of Education, Shandong University, Jinan 250061, China
e-mail: msli@sdu.edu.cn

X.-C. Wang
New Material Institute of Shandong Academy of Sciences, Jinan 250014, China

K.-H. Ding, S.-L. Cui, Y.-C. Sun
Yantai Shougang Magnetic Materials Inc, Yantai 265500, China

1 Introduction

Since invented in the 1980s, sintered Nd–Fe–B magnet has been widely used in many kinds of permanent magnet motors, due to their excellent magnetic properties such as high remanence, coercivity and maximum energy product [1–4]. However, the sintered Nd–Fe–B magnet is fragile to corrosion under various environments, which causes surface degradation and pulverization of these materials and greatly limits its application [5]. Over the past few decades, extensive efforts have been carried out on the corrosion prevention of the Nd–Fe–B magnet. The sintered Nd–Fe–B magnet is composed of matrix-phase $\text{Nd}_2\text{Fe}_{14}\text{B}$, precipitated Nd-rich phase and B-rich phase along grain boundary [6, 7]. The different potentials of the each phase will inevitably lead to electrochemical reaction in the humid environment. With the grain boundary phases as the anode and the matrix phase as the cathode, small size of the grain boundary phase under the effect of anode current will accelerate corrosion, causing intergranular corrosion [8].

There are mainly two methods to improve the corrosion resistance of the sintered Nd–Fe–B magnet so far. One is adding alloying elements such as Co, Dy and Ni to alter the intrinsic anti-corrosion property of the magnet [9–12]; the other is applying protective coatings on the surface of the magnet [13–16]. The limited improvement in corrosion resistance through the former method was found, accompanied with a sacrifice of magnetic properties and an increase in the cost [17]. In contrast, the surface protection technology is simple and can significantly improve the corrosion resistance. It becomes the main method of surface-corrosion-resistant treatment on the sintered Nd–Fe–B magnet.

In terms of chemical conversion coating for this kind of magnet, chromating is used for anti-corrosion and has good effect. But this treatment generated toxic and carcinogenic products. Therefore, the other types of environmentally friendly conversion coatings were studied in order to replace chromate coatings due to the toxicity of Cr^{6+} . The phosphate chemical conversion (PCC) is a process to form phosphate coating on metal surface through chemical and electrochemical reactions [18]. It is an economic, simple and environmentally friendly surface treatment technology which can improve the corrosion resistance of the materials. The application of phosphate anti-corrosion technology on steel material is already mature [19, 20], while few were adopted for the sintered Nd–Fe–B magnet.

In this study, a homogeneous phosphate coating was prepared on the surface of the sintered Nd–Fe–B magnet by PCC method. The morphology, phase composition and thickness of the top coatings on the surface of the magnet were investigated by field emission scanning electron microscopy (FE-SEM), energy-dispersive spectrometer (EDS), Fourier transform infrared spectrometer (FTIR) and coating thickness gauge. The corrosion behaviour of the magnet was evaluated by copper drip method, neutral salt spray method and electrochemical potentiodynamic polarization experiment. The magnetic properties of the phosphated magnet were also tested. This research provides an important phosphate treatment technique to increase the corrosion resistance of the Nd–Fe–B magnet.

2 Experimental

2.1 Materials and chemical conversion process

Commercially N45M-sintered Nd–Fe–B magnet was used with the size of $\Phi 10 \text{ mm} \times 8 \text{ mm}$. Figure 1 shows the phosphate process. The specimens were abraded with emery paper and polished, followed by a degreasing procedure in an alkaline solution at $60 \text{ }^\circ\text{C}$ for 15 min. Then, they were rinsed ultrasonically in acetone and ethanol, respectively. Pickling was performed on the specimens at room temperature for 2 min. After ultrasonic cleaning with deionized water several times, the samples were immersed in the PCC bath at $90 \text{ }^\circ\text{C}$ for 20 min. After the PCC

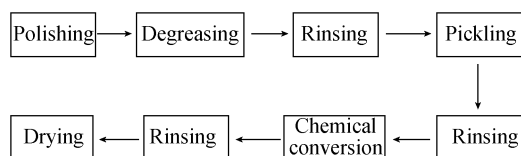


Fig. 1 Schematic diagram for technological process of chemical conversion method

treatments, the coupons were washed with deionized water and dried in warm air stream.

2.2 Measurement and characterization

2.2.1 Surface morphology and composition of phosphate coatings

The macro-morphology of the PCC coatings on the sintered Nd–Fe–B magnet was observed in natural light, and the microstructure and composition were examined using FE-SEM (SU-70 model made in Japan) equipped with EDS. Furthermore, a BRUKER TENSOR 37 model of FTIR spectrometer was utilized to characterize functional groups of the coatings within the spectra range of $4000\text{--}400 \text{ cm}^{-1}$. The specimens for FTIR analysis were prepared with a powder mixture of PCC coatings scraped off Nd–Fe–B magnet and KBr.

2.2.2 Thickness measurement of phosphate coatings

In order to determine the scope of the coating thickness distribution, mini-test coating thickness gauge (600B FN2 model) was employed to test multipoint thickness of the PCC coatings. The thickness measurement was conducted on three phosphated specimens numbered by Samples 1, 2 and 3 in the same batch. Five testing points were picked near the centre of each specimen.

2.2.3 Corrosion resistance test of phosphate coatings

The corrosion resistance of the PCC coatings were investigated by copper drip method (GB/T 6807-2001), neutral salt spray test (GB/T 10125-1997) and electrochemical potentiodynamic polarization experiments.

1 L copper sulphate drip solution was prepared by 41.0 g $\text{CuSO}_4 \cdot 5\text{H}_2\text{O}$, 35.0 g NaCl and 13.0 ml hydrochloric acid solution ($0.10 \text{ mol} \cdot \text{L}^{-1}$). At room temperature, a drop of the copper sulphate solution was added on the dried surface of the phosphate specimens, the time required for the solution turned earthy red was observed, and the average value of three samples was taken.

The salt spray test machine (YWX/Q-150 model) was utilized for the neutral salt spray test. The testing temperature was $35 \text{ }^\circ\text{C}$, and testing solution was 5 wt% sodium chloride solution with $\text{pH} = 7$, intake pressure of 0.3 MPa, spray pressure of 1.0 MPa and spray flow rate of $1 \text{ ml} \cdot \text{h}^{-1}$. The phosphated and no phosphated specimens were used for the salt spray test simultaneously, and the corrosion time was recorded. A group specimen in interval of 1 min was taken to obtain the exact duration of different samples in the neutral salt fog corrosion.

The corrosion characteristic curves of the phosphate coatings were measured through a Parstat 2273 model of potentiodynamic polarization station with a three-electrode set-up in 3.5 wt% NaCl aqueous solution at a scan rate of $10 \text{ mV}\cdot\text{s}^{-1}$. The saturated calomel electrode (SCE), platinum and the sample coupon with 0.785 cm^2 exposed area were used as reference, counter and working electrodes in the three-electrode cell, respectively.

2.3 Magnetic test of phosphate coatings

To study the effect of the PCC coating on the magnetic properties of the Nd-Fe-B magnet, the remanence (B_r), coercive force (H_{c_j}) and square degree (H_k/H_{c_j}) of the phosphated and no phosphated specimens were tested by a NIM-2000 model of magnetic characteristic detector.

3 Results and discussion

3.1 Surface morphology and structure of phosphate coatings

As shown in Fig. 2a, a layer of dense grey coatings can be observed on the surface of Nd-Fe-B magnets with naked

eye under the natural light after PCC treatment. Figure 2b, c shows FE-SEM images of phosphate coatings. It can be seen that the coatings are granular with a grain size of 3–10 μm . The PCC coatings are uniform and dense on the surface of the sintered Nd-Fe-B magnet, and there are no bare substrates. Figure 2d shows the EDS result of Point A in Fig. 2c. As a comparison, the EDS result of the Nd-Fe-B substrate is shown in Fig. 2e. It reveals that the PCC coatings contain such elements as Zn, Mn, P, O and other metal and nonmetallic ones.

Figure 3 shows FTIR spectra of the phosphate coatings and Nd-Fe-B substrates. The FTIR spectra present the typical absorption peaks of the PO_4^{3-} group around 1056 cm^{-1} corresponding to the P=O stretching vibration mode. This indicates the coatings with phosphate structurally. Furthermore, the peaks are attributed to O-H bending (1522 and 1645 cm^{-1}) and O-H stretching (3737 and 3858 cm^{-1}), respectively, implying the existence of some crystal water.

3.2 Thickness of phosphate coatings

Table 1 and Fig. 4 show the thickness distribution of phosphate coatings. It can be seen that the thickness range of the coatings on the surface of sintered Nd-Fe-B magnet is between 10 and 18 μm . This is a suitable thickness for

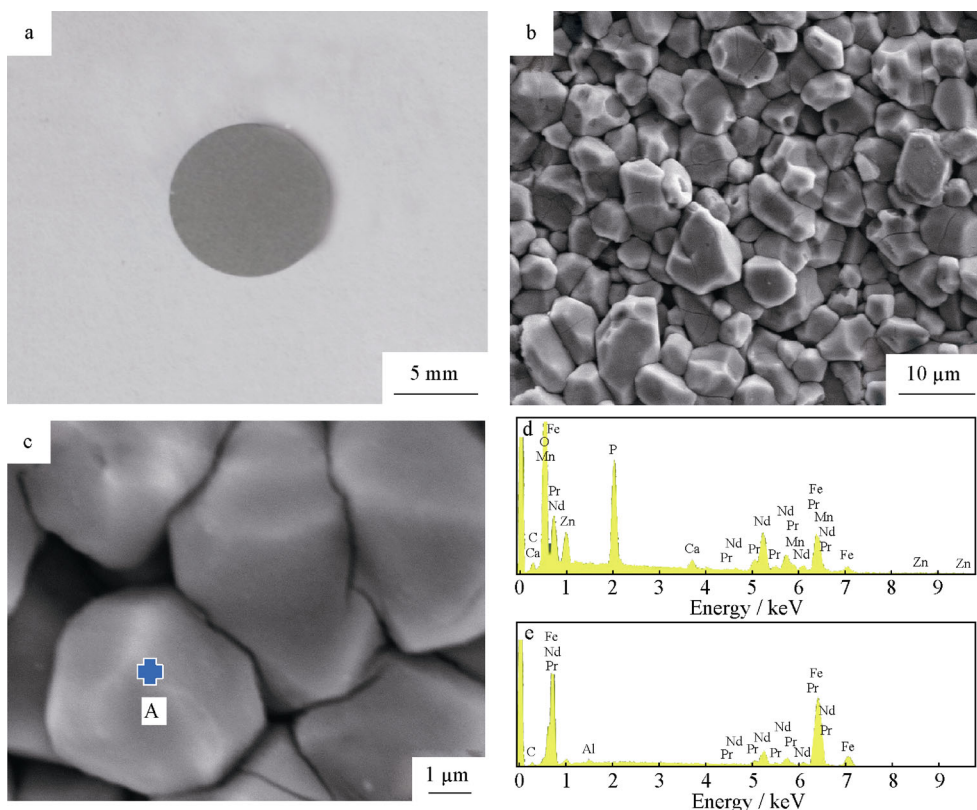


Fig. 2 Morphologies and compositions of PCC coatings on surface of sintered Nd-Fe-B magnet: **a** macroscopic morphology; **b**, **c** FE-SEM images with different magnifications; **d** EDS result of PCC coatings and **e** EDS result of Nd-Fe-B substrate

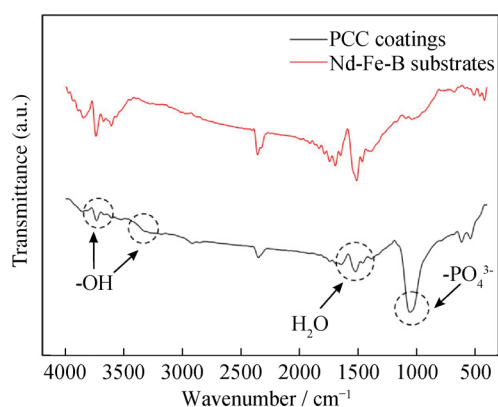


Fig. 3 FTIR spectra of Nd-Fe-B substrate and PCC coatings on surface of magnet

Table 1 Thickness of PCC coatings on surface of sintered Nd-Fe-B magnet with five testing points (μm)

Samples	Point 1	Point 2	Point 3	Point 4	Point 5
1	12	14	12	13	14
2	10	13	11	16	13
3	17	14	18	16	15

the anti-corrosion of Nd-Fe-B magnet. If the PCC coating is too thin, it cannot supply a good protection for the substrate because of the porous structure of the magnet. In contrast, if the PCC coating is too thick, it will affect the magnetic properties of the magnet.

3.3 Corrosion resistance of phosphate coatings

The copper drip test indicates that the discoloured time of the testing solution on the phosphated specimens is 24 s, but only 1–2 s on the no phosphated specimens. It can be seen that the corrosion resistance of the Nd-Fe-B magnet is improved significantly after PCC treatment.

The corrosion resistances of the phosphated and no phosphated specimens under the same condition of the neutral salt spray were tested by the salt spray test chamber. As shown in Fig. 5, the significant corrosion colour appears on the surface of the no phosphated specimens after only 2 min, while there is no change for the phosphated specimens. The corrosion colour on the phosphated specimens appears after 12 min. The phosphated and no phosphated specimens were treated by immersion oil method, respectively. Then, the salt spray testing results show that the corrosion colour appears on the no phosphated specimens only after 30 min, but on the phosphated specimens after 3 h. The phosphate coating on the sintered Nd-Fe-B magnet can supply an effective protection in neutral salt spray conditions.

Figure 6 is the potentiodynamic polarization curves in 3.5 wt% NaCl solution of phosphated and no phosphated sintered Nd-Fe-B magnets. The corresponding

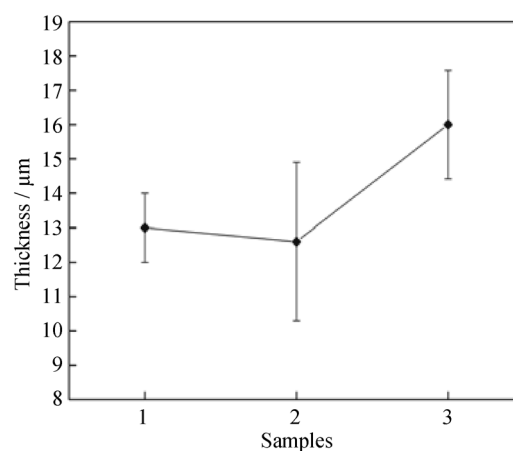


Fig. 4 Average thickness and deviation of phosphate coatings



Fig. 5 Macro-photographs of phosphated and no phosphated samples at 2 min in salt spray test

electrochemical parameter fitting results are shown in Table 2. As seen from Fig. 6 and Table 2, compared with those of the Nd-Fe-B substrate, the corrosion potential (E_{corr}) of the phosphate specimens increases, but the corrosion current (I_{corr}) decreases greatly. Thus, the Nd-Fe-B magnet is prone not to raise corrosion, but to noticeably slow the velocity in the event of corrosion after preparation of phosphate coatings on its surface.

3.4 Magnetic properties before and after phosphate treatment

In order to know the effect of the phosphate coatings on the magnetic properties of the Nd-Fe-B magnets, the remanence (B_r), coercive force ($H_{\text{c}j}$) and the square degree ($H_k/H_{\text{c}j}$) of phosphated and no phosphated specimens were tested by the magnetic characteristic detector. The testing results are shown in Table 3. It can be seen that the

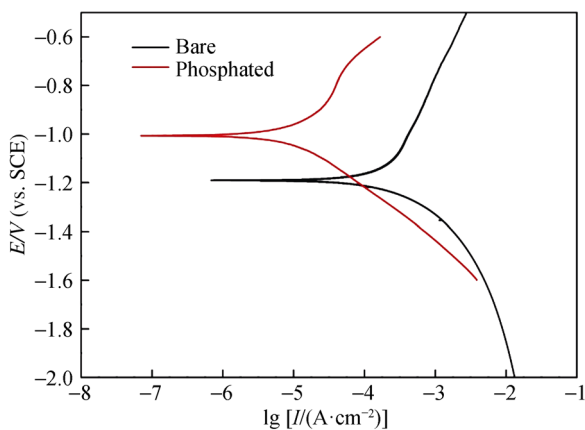


Fig. 6 Potentiodynamic polarization curves of phosphated and no phosphated Nd–Fe–B magnets

Table 2 Self-corrosion potentials and corrosion currents of phosphated and no phosphated Nd–Fe–B magnets

Samples	$E_{\text{corr}}/\text{mV}$ (vs. SCE)	$I_{\text{corr}}/(\mu\text{A}\cdot\text{cm}^{-2})$
No phosphated	−1192	30.58
Phosphated	−1007	1.70

Table 3 Magnetic properties of phosphated and no phosphated Nd–Fe–B magnets

Samples	$H_{\text{cj}}/(\text{kA}\cdot\text{m}^{-1})$	B_{r}/T	$H_{\text{k}}/H_{\text{cj}}$
No phosphated	1334.92	1.33	0.98
Phosphated	1323.79	1.33	0.97

magnetic properties of the two kinds of the specimens are similar. This suggests that PCC treatment has few effects on the magnetic properties of sintered Nd–Fe–B magnet.

4 Conclusion

The uniform phosphate coatings with a thickness range of 10–18 μm were prepared on the sintered Nd–Fe–B magnets. The coatings are composed of Fe, Mn, and Zn phosphates with a crystal size of 3–10 μm . The Nd–Fe–B substrates are fully covered with the phosphate coatings after the chemical conversion treatment at 90 °C for 20 min. Compared with the no phosphated Nd–Fe–B magnets, the phosphated ones show a better corrosion resistance and unchanged magnetic properties. Therefore, the PCC treatment can be used as an effective and simple way to improve the corrosion resistance of the sintered Nd–Fe–B magnets.

Acknowledgments This work was financially supported by the China National Major Special Project for the Rare Earth and Rare Metallic Materials (No. (2012) 1743).

References

- [1] Sagawa M, Hirosawa S, Yamamoto H, Fujimura S, Matsuura Y. Nd–Fe–B permanent magnet materials. *Jpn J Appl Phys*. 1987;26(6):785.
- [2] Schultz L, El-Aziz AM, Barkleit G, Mummert K. Corrosion behaviour of Nd–Fe–B permanent magnetic alloys. *Mater Sci Eng A*. 1999;267(2):307.
- [3] Jiang CB, An SZ. Recent progress in high temperature permanent magnetic materials. *Rare Met*. 2013;32(5):431.
- [4] Wu Q, Zhang PY, Pan MX, Li DY, Ge HL. Crystallization kinetics and magnetization behavior of $\text{RE}_{3.5}\text{Fe}_{66.5}\text{Co}_{10}\text{B}_{20}$ (RE = Pr, Nd) nanocomposite ribbons. *Rare Met*. 2014;33(6):681.
- [5] Man HH, Man HC, Leung LK. Corrosion protection of NdFeB magnets by surface coatings—Part 2: electrochemical behaviour in various solutions. *J Magn Magn Mater*. 1996;152(1):47.
- [6] Li WF, Ohkubo T, Hono K. Effect of post-sinter annealing on the coercivity and microstructure of Nd–Fe–B permanent magnets. *Acta Mater*. 2009;57(5):1337.
- [7] Tsubokawa Y, Shimizu R, Hirosawa S, Sagawa M. Effect of heat treatment on grain-boundary microstructure in Nd–Fe–B sintered magnet. *J Appl Phys*. 1988;63(8):3319.
- [8] Minowa T, Yoshikawa M, Honshima M. Improvement of the corrosion resistance on Nd–Fe–B magnet with nickel plating. *IEEE Trans Magn*. 1989;25(5):3776.
- [9] Rieger G, Seeger M, Sun Li, Kronmuller H. Micromagnetic analysis applied to melt-spun NdFeB magnets with small additions of Ga and Mo. *J Magn Magn Mater*. 1995;151(1):193.
- [10] Tokuhara K, Hirosawa S. Corrosion resistance of Nd–Fe–B sintered magnets. *J Appl Phys*. 1991;69(8):5521.
- [11] Sagawa M, Tenaud P, Vial F, Hiraga K. High coercivity Nd–Fe–B sintered magnet containing vanadium with new microstructure. *IEEE Trans Magn*. 1990;26(5):1957.
- [12] Hirosawa S, Mino S, Tomizawa H. Improved corrosion resistance and magnetic properties of Nd–Fe–B sintered magnets with Mo and Co. *J Appl Phys*. 1991;69(8):5844.
- [13] Bala H, Pawlowska G, Szymura S, Rabinovich YM. Electrochemical corrosion characterisation of intermetallic phases occurring in Nd–Fe–B type magnets. *Br Corros J*. 1998;33(1):37.
- [14] Pierri E, Tsamouras D, Dalas E. Ferric phosphate precipitation in aqueous media. *J Cryst Growth*. 2000;213(1):93.
- [15] Costa I, Sayeg II, Faria RN. The corrosion protection of RE-iron-boron magnets by a phosphate treatment. *IEEE Trans Magn*. 1997;33(5):3907.
- [16] Qin CD, Li ASK, Ng DHL. The protective coatings of NdFeB magnets by Al and Al (Fe). *J Appl Phys*. 1996;79(8):4854.
- [17] Man HH, Man HC, Leung LK. Corrosion protection of NdFeB magnets by surface coatings—Part I: salt spray test. *J Magn Magn Mater*. 1996;152(1):40.
- [18] Tamborim Takeuchi SM, Azambuja DS, Costa I. Cerium conversion layer for improving the corrosion resistance of phosphated NdFeB magnets. *Surf Coat Tech*. 2006;201(6):3670.
- [19] Hawthorne HM, Neville A, Troczynski T, Hu X, Thammachart M, Xie Y, Fu J, Yang Q. Characterization of chemically bonded composite sol–gel based alumina coatings on steel substrates. *Surf Coat Tech*. 2004;176(2):243.
- [20] Fujioka E, Nishihara H, Aramaki K. The inhibition of passive film breakdown on iron in a borate buffer solution containing chloride ions by mixtures of hard and soft base inhibitors. *Corros Sci*. 1996;38(10):1915.